ELSEVIER

Journal of Hazardous Materials 53 (1997) 93–114

JOURNAL OF HAZARDOUS MATERIALS

Gas build-up within a single building volume — comparison of measurements with both CFD and simple zone modelling

S. Gilham [a], D.M. Deaves [a,*], R.P. Hoxey [b], C.R. Boon [b], A. Mercer [c]

[a] *WS Atkins Safety & Technology, Woodcote Grove, Ashley Road, Epsom, Surrey, KT18 5BW, UK*
[b] *Silsoe Research Institute, Wrest Park, Silsoe, Bedfordshire, MK45 4HS, UK*
[c] *UK Health & Safety Executive (HSE), Broad Lane, Sheffield, S3 7HQ, UK*

Received 10 January 1996; accepted 25 June 1996

Abstract

When gas is released into a building, it will begin to disperse under the action of its own momentum and buoyancy, and of any pre-existing ventilation flows. For small releases, even slight ventilation may reduce the gas concentration below dangerous (e.g. flammable) limits, whereas, at the other extreme, large releases could result in a breach of containment, and hence would be only slightly affected by the presence of the building. For intermediate-scale releases, which are of interest in risk assessments, the nature of the build-up and movement within the building, along with the size and locations of any openings, will determine the rate at which gas is released to the environment. This study was undertaken as part of an ongoing research effort to enable effects of buildings on gas build-up, and subsequent release to the environment, to be calculated with greater confidence. Existing techniques for such calculations tend to use the assumption of complete mixing within the volume at any given time, thus enabling transient release rates from the building to be determined. Whilst this may be appropriate for high-momentum releases, it is clearly too simplistic for general application. Measurements of the build-up of CO_2, released within a simple cube of side 2.4 m, have, therefore, been undertaken in the test facility at the Silsoe Research Institute, and compared with the results from both CFD and zone modelling. Provided that care is taken in their application, these models both produce reasonable comparisons with the experimental data. © 1997 Elsevier Science B.V.

Keywords: CFD; Gas build-up; Simple zone modelling

* Corresponding author. Tel: (44-1372) 726410; fax: (44-1372) 740055; telex: 266701 (Atkins G).

PII S0304-3894(96)01836-5

1. Introduction

The effects of accidental releases of hazardous vapours will depend upon the extent to which they are dispersed in the atmosphere. The dispersion mechanisms for flat unobstructed terrain are well known, and a range of models is available to enable dispersion predictions to be made. In order to make appropriate use of such models, it is necessary to provide a realistic source term. In the case where the release may occur within a building, (such as potential releases of chlorine at many water treatment plants), the effective source term may differ rather from the actual rate of release from pipework, evaporating pools etc.

In order to address this particular source term problem, HSE commissioned WS Atkins to undertake studies investigating the use of CFD for internal dispersion flows. The initial phase of the work [1] reviewed previous CFD work, and also identified simpler 'zone' models, in which certain assumptions are made concerning the mixing, and analytical, or semi-analytical, solutions are obtained. In most cases, these models were developed in order to determine concentration within the building, either from a building safety point of view, or to enable ventilation comfort criteria to be met. The only such modelling currently used for source term calculation [2] makes the assumption of uniform mixing within the building.

Considerable CFD development and modelling, and some further simple modelling, were both the subject of the second phase of the work [3]. The CFD runs undertaken have allowed optimisation of features such as mesh definition and turbulence modelling, by comparing predictions with validation data. Since it was found that data were available only either for low release rates, with negligible momentum and only slight jet-induced mixing, or for high-pressure jets with almost complete mixing, it was decided to obtain further data relating to the intermediate case in which there is some mixing, but it is by no means complete.

The experimental set up is described and results presented in the next section. This is followed by separate sections on the modelling of internal gas dispersion flows either using simple ventilation principles (Section 3) or CFD modelling (Section 4). A comparison between these two techniques and the physical modelling results is then given, followed by the overall conclusions of this study.

2. Experimental results

2.1. Facility

The Building Section under consideration has floor dimensions 11.7×3 m, with a pitched roof such that the height varies from 1.85 m at the eaves to 3.3 m at the ridge. It is currently configured with an extract fan at each side wall, and a ventilation inlet at the apex, beneath which is a deflector plate. The flow is therefore strongly driven by the forced ventilation, which sets up a large recirculation cell in each symmetric half of the building.

2.2. Geometry

A 2.44 m cube was constructed at Silsoe Research Institute, as shown in Fig. 1, and was totally enclosed within the Building Section, so that the internal flow was unaffected by external environmental conditions.

The front of the cube and two of its sides were constructed of perspex in order that non-intrusive flow visualisation could be undertaken. The gas inlet position was located at the centre of one of the vertical faces, and two closable vents were formed at the top and bottom of the same face. These measured 0.2×0.05 m, and were designed to allow sufficient venting to avoid over-pressurisation. During the tests, either one or both vents were left open, to enable their effects upon the flow to be determined.

2.3. Release conditions

Carbon dioxide was used as the contaminant gas, and was injected into the room at ambient conditions. To ensure that this was achieved, the gas, 100% carbon dioxide, was pre-released into a large polythene bag, of circumference 2 m and length approximately 15 m. The bag was situated in the temperature-controlled outer shell of the Building Section, and thus equilibrated to the air temperature in and around the test cube before release was initiated.

The gas was pumped from the bag with a fan unit, capable of delivering up to 1400 $l\,min^{-1}$, to the chamber at the rates specified (inlet gas speeds 5 $m\,s^{-1}$ and 8 $m\,s^{-1}$). With the quantity of gas stored in the bag (maximum approximately 4.5 m^3), these values allowed the gas to be pumped for 5 min and 3 min, respectively. In practice, although the ambient temperature was reached, this intermediate storage introduced some dilution to the CO_2, so that it was emitted at source concentrations of 70–80%.

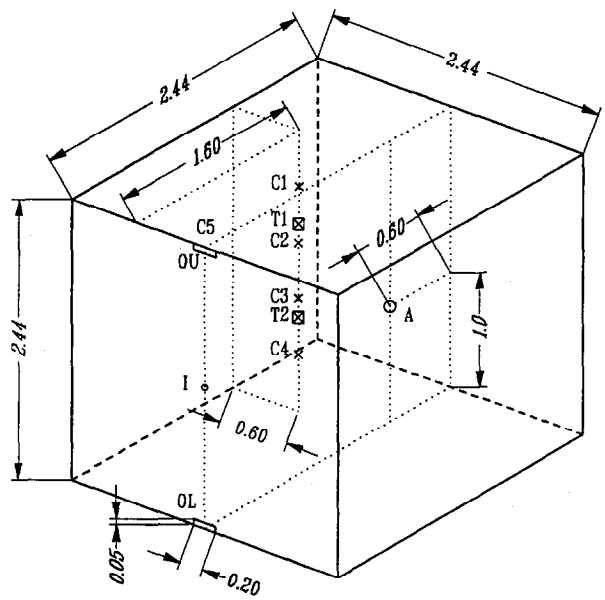

Fig. 1. Experimental chamber showing sensor locations.

To ensure fully developed flow, the final portion of the tubing was a rigid pipe, 1 m long and 50 mm in diameter, the end of which was the inlet orifice. This terminated flush with one of the walls, giving a jet which was directed horizontally towards the centre of the room.

2.4. Inlet flow rate

Two inlet mean speeds of the gas were required, 5 $m s^{-1}$ and 8 $m s^{-1}$, giving flow rates, with the 50 mm diameter inlet, of 600 $l min^{-1}$ and 950 $l min^{-1}$. These were chosen to provide the appropriate mixing conditions, rather than to be representative of any specific types of release.

The settings of flow were made with air using standard rotameters. Because of the higher density of carbon dioxide, the rotameters will give higher flow readings at high concentrations of the gas. Therefore, in order to check the speed at the inlet, this was measured, with carbon dioxide, using a rotating vane anemometer; effective discharge coefficients were not determined.

The inlet flow rate was checked by placing the rotating vane anemometer at the upper outlet of the box to ensure that it was always measuring flow in air. For the experiments with the upper outlet only open, it was possible to obtain an indication of the rate, bearing in mind that the outlet was rectangular and therefore flow was non-uniform. The flow rate determined in this manner was within 10% of the rate measured by rotameters, which was considered acceptable.

2.5. Carbon dioxide concentrations

The instruments used, ADC (Analytical Development Company) Infra-red Gas Analysers, and their sampling locations, are listed in Table 1. The vertical array on which C1–C4 were mounted was positioned out of the gas jet at 1.6 m from the left wall and 0.6 m from the rear wall, and C5 was located at the upper outlet OU (see Fig. 1).

All these instruments were located in the Building Section control room. The gas lines from the chamber to each analyser were of the same length which, with a 0.5 $l min^{-1}$ gas sampling rate, means that the output from the analysers was phase shifted in time by 40 s. The real-time zero data were thus at the 40 s mark in the logged data.

2.6. Temperature

Temperatures were measured at five locations. Two copper–constantin thermocouples in the chamber, T1 and T2, were mounted on the instrument array (see Fig. 1)

Table 1
Deployment and characteristics of gas sensors

Position	Scale (% CO_2)	Height from floor (m)	
		(Runs 3–5)	(Runs 6–8)
C1	5	1.70	1.95
C2	25	1.34	1.46
C3	100	0.98	0.98
C4	100	0.48	0.49
C5	0.5	2.40	2.40

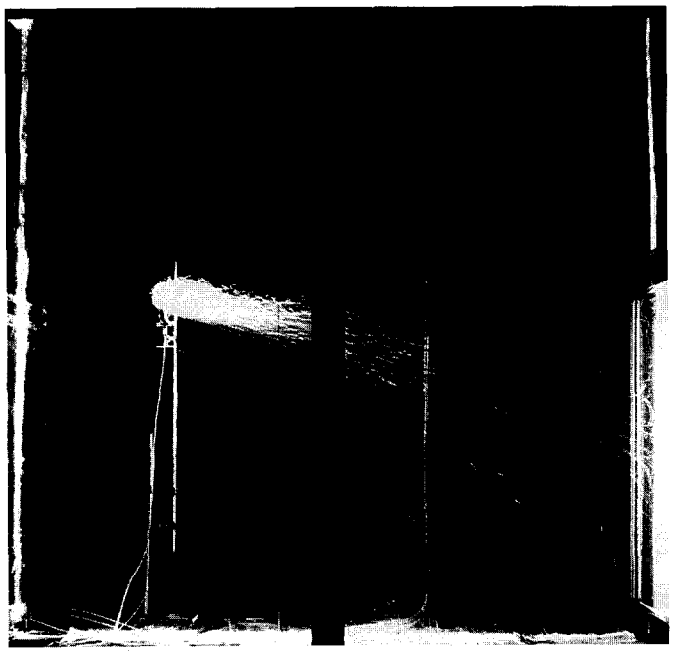

Fig. 2. Carbon dioxide jet (5 $m s^{-1}$ inlet speed).

and were at 1 m and 1.75 m from the floor. The temperature of the gas as it was pumped into the chamber was also monitored with a thermocouple. The air temperature in the Building Section outer shell, at one position near the carbon dioxide bag, was measured with a Rotronics OP200 Temp/RH probe. These two measurements were taken to check that isothermal conditions were maintained.

The temperature around the outside of the chamber was also monitored for the same purpose, using a Rotronics OP200 probe.

Table 2
Release conditions for Runs 3–9

Run	Rel. rate ($l min^{-1}$)	Duration (min)	Inlet conc. (%)	Vent regime	Layer concentration (%)	Normalised layer conc. (%)
3	600	5	70	U	25	36
4	600	5	70	U+L	23.5	34
5	600	5	75	L	24	32
6	950	3	80	L	23	29
7	950	3	80	U+L	23	29
8	950	3	80	U	24.5	31
9	600	5	70	U	24	34

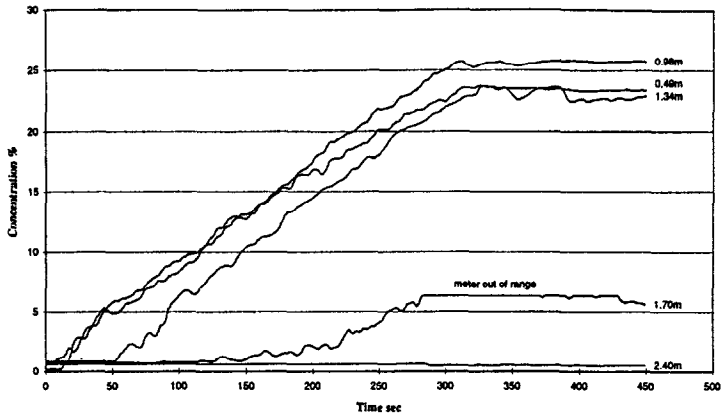

a) Upper vent only open (Run 3)

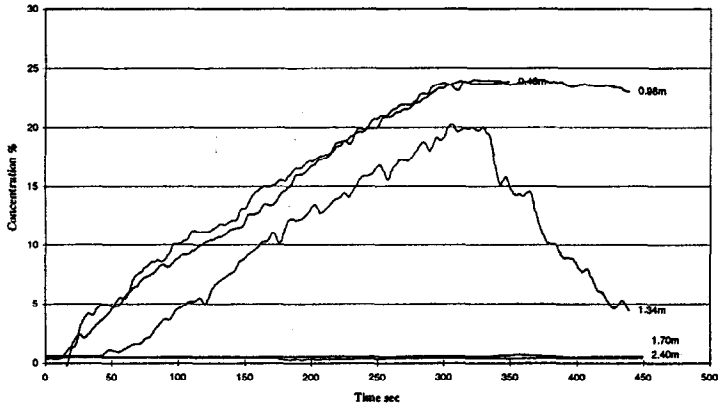

b) Upper and lower vents open (Run 4)

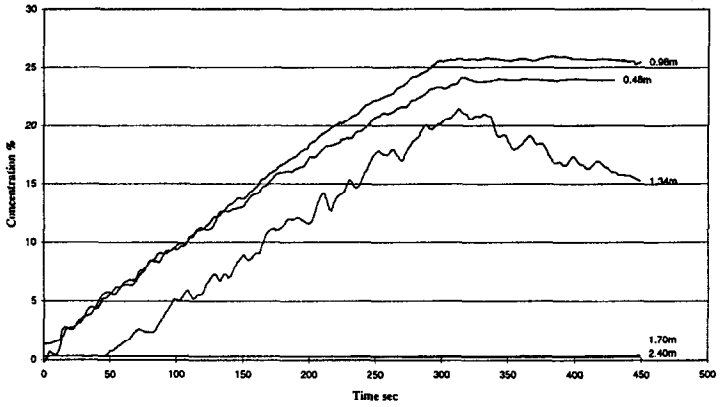

c) Lower vent only open (Run 5)

Fig. 3. Experimental CO_2 concentration time history.

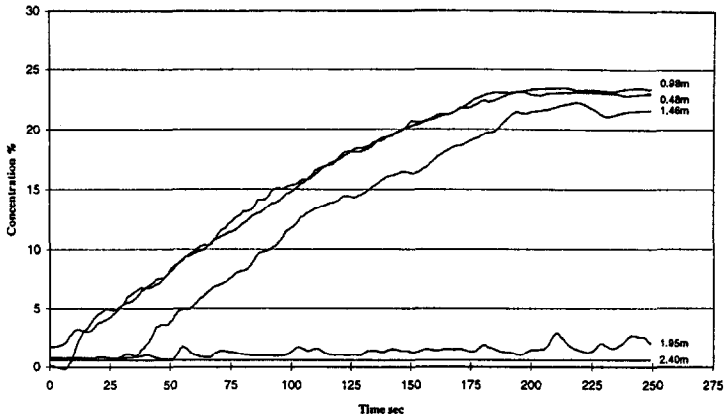

a) Lower vent only open (Run 6)

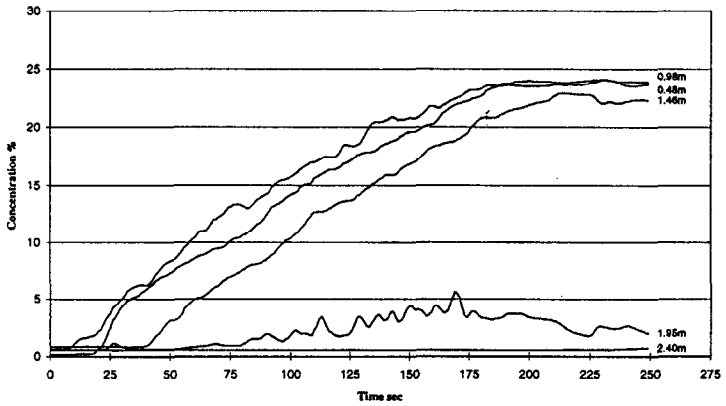

b) Upper and lower vents open (Run 7)

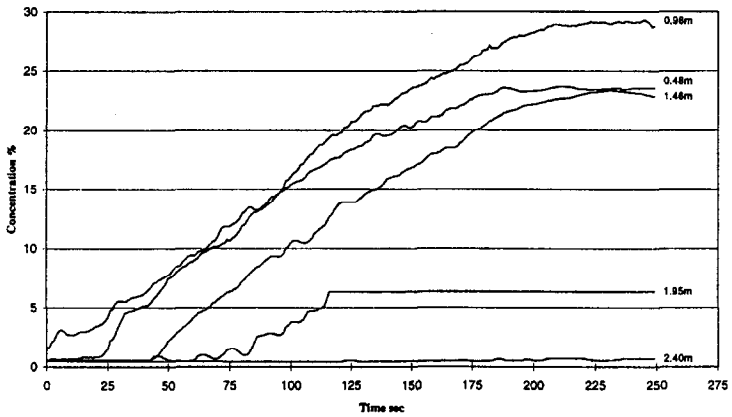

c) Upper vent only open (Run 8)

Fig. 4. Experimental CO_2 concentration time history.

2.7. Jet velocities

To give an indication of the speed and direction of the jet, a Gill Ultrasonic Research Anemometer was located on the centre line of the jet, 1 m from the floor and 0.6 m from the right hand wall (Fig. 1).

2.8. Flow visualisation

Visualisation of the jet was achieved by injecting liquid film bubbles into the chamber, illuminating them with a 150 mm wide vertical slice of light along the line of the jet, and photographing the result. The resulting pictures showed the clear downward bending of the dense jet, as seen in Fig. 2 (for the same release conditions as Run 3).

2.9. Gas build-up results

It was observed that the inlet gas concentration was less than 100% for each run undertaken. Measurements indicated a slight variation of concentration with time, amounting to around 10–15% over the duration of the release. The temperature at the inlet was also measured, and remained steady (within around 1°C) over the release duration, demonstrating the good achievement of isothermal conditions. Further analysis of the results was therefore based on the assumption of constant inlet temperature and concentration, the latter being taken as an average over the release duration.

The first two runs were preliminary tests, designed to ensure the correct operation of the system. Runs 3–5 then used the low flow rate for various opening configurations, while Runs 6–8 were for a high flow rate. Run 9 was a further run at a low flow rate with a release rate of 600 $l\,min^{-1}$ for 5 min, i.e. notionally equivalent to Run 3. 'Steady state' conditions were achieved (the lower outlet was closed and thus the box retained all the CO_2) and the concentration as a function of height was investigated. From the results, by integrating the resulting concentration profile, the quantity of gas released into the box was estimated at approximately 2.3 m^3. The inlet gas concentration was approximately 70%, and, thus, given the above release conditions, the quantity determined by this method is approximately 2.1 m^3. The two methods give values to within 10%, which is considered acceptable for this type of experiment.

For each of the two release rates, three different vent conditions were used, to

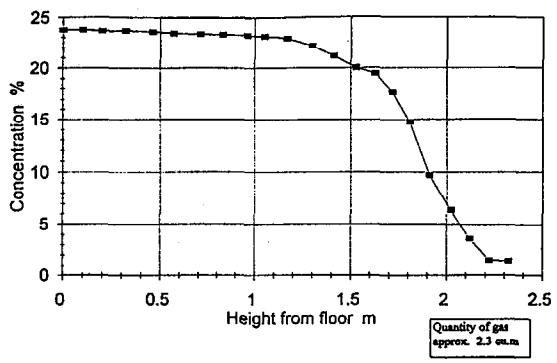

Fig. 5. Experimental CO_2 concentration profile, 70% at 600 $l\,min^{-1}$ upper vent only open, steady state.

determine the effect of the vents on the build-up. The conditions are summarised in Table 2, in which U indicates that the upper vent only was open, L that the lower vent only was open and U + L that both were open. The last column gives the final concentration relative to that at inlet.

The build-up of concentration for each of these runs was recorded and is shown in Figs. 3 and 4 for Runs 3–5 and Runs 6–8, respectively. The results of the quasi-'steady-state' Run 9 are presented in Fig. 5, which demonstrates the clear existence of a well-mixed layer of depth about 1.5 m, although the top does not represent a sharp concentration interface.

3. The application of simple modelling

3.1. Internal flow structure

An intensive series of low release-rate positively and negatively buoyant gas build-up tests was undertaken by British Gas and has been incorporated into a simple zone model [4]. This was developed primarily to determine the distribution of gas within a building, rather than the location and rate of any release from a building. For the applications considered here, the internal flow structure is only relevant insofar as it affects the outflow. In spite of this, the Cleaver model was used as the most appropriate for the cases considered.

In the model, two key dimensionless parameters were identified which determine the way in which the internal build-up is likely to occur, namely the volume Richardson number and the overturning number.

3.1.1. Volume Richardson number

$$Ri_v = \frac{V^{1/3} g'_o}{u_o^2} \tag{1}$$

where

V = volume of enclosure

$g'_o = g(\rho_g - \rho_a)/\rho_g$

u_o = velocity of jet release

ρ_a = density of air

ρ_g = density of gas at inlet

In the Silsoe tests, $V = 2.44^3 = 14.5$ (m^3), $u_o = 5$ m s^{-1} (Runs 3–5) or 8 m s^{-1} (Runs 6–8), $\rho_g = \rho_a + c(\rho_c - \rho_a)$, where ρ_c = density of pure CO_2, and c = concentration of CO_2 at inlet. This gives

$Ri_v = 0.26$ Runs 3 – 5

$= 0.11$ Runs 6 – 8

According to Cleaver et al., this parameter provides some measure of the ability of the jet to promote mixing within the enclosure. They use a considerable volume of data

from natural gas releases to demonstrate the scaling of an 'additional mixing depth' (δ) against Ri_v, such that, for horizontally directed releases

$$\delta = 40 r_o / \sqrt{Ri_v} \tag{2}$$

where

r_o = radius of jet source (= 0.025 m)

Hence

$\delta = 2.0$ m Runs 3 – 5
$= 3.0$ m Runs 6 – 8

It should be noted that there is considerable scatter in the data, such that the constant of proportionality (40) may be uncertain to within half an order of magnitude, which could therefore give δ of 1.0 m or less.

3.1.2. Overturning number

The momentum flux M_c and buoyancy force B_c are compared to determine the stability of any gas layer which forms beneath the ceiling (buoyant gas) or above the floor (dense gas); their ratio is the overturning number, Ω. The definitions are:

$$M_c = \rho \pi r^2 u^2 \tag{3}$$

$$B_c = A r \Delta \rho g \tag{4}$$

$$\Omega = M_c / B_c \tag{5}$$

Where

A = horizontal cross – sectional area of building
$\rho, \Delta\rho$ are local density and density differences as the plume strikes the floor/ceiling
r, u are local plume radius and velocity.

The values of these parameters are difficult to predict within the flow being considered. However, in order to determine approximate orders of magnitude, it is assumed, to a first approximation, that the inlet jet is unaffected by buoyancy. In that case,

$r \sim z$
$u \sim 1/z$ where z is distance along jet centre – line
$\Delta\rho \sim c \sim 1/z$

Hence B_c and r^2u^2 are both constant, while (M_c), and therefore Ω, decreases with z, since $\rho = \rho_a(1 + c(\rho_g - \rho_a))$. In the present case, taking a path length of 2.5 m gives

$\Omega = 0.1$ Runs 3 – 5
$= 0.22$ Runs 6 – 8

It is noted that these values are on the border of acceptability for the application of Cleaver's model. Nevertheless, applying the simple model then gives a gas/air mixture layer depth (h_1) which reaches $0.5 z_r$ (z_r = release height or depth) at $\Omega = 0.1$, and increases to min(0.5 $z_r + \delta$, H), where H = height of room (m), at $\Omega = 0.3$. Thus:

$h_1 = 0.6$ Runs 3 – 5
$= 1.68$ Runs 6 – 8

The exact magnitude of h_1 is clearly very sensitive to Ω in this case, and it is noted that the value of Ω is also subject to some uncertainty unless detailed modelling (such as CFD) is undertaken.

It is noted that Cleaver's work could also be interpreted such that z_r = travel distance (= 2.4 m). In that case, h_1 would be calculated as 1.2 m for Runs 3–5 and 1.92 m for Runs 6–8. This emphasises the difficulties of and uncertainties in determining h_1 for the particular cases under consideration; the values derived above should therefore be treated as indicative only.

3.2. Transient nature of gas build-up

The analysis of Cleaver et al., and the data used to support it, applies to volumes which are effectively sealed, apart from pressure relief, so that no gas or gas/air mixture is able to emerge. A significant concern within the study undertaken for HSE relates to the time-dependent emission of gas/air mixture from a building in which a gas release has taken place. This emission 'profile' is dependent upon the various parameters involved, in particular the size and location of openings. Simple modelling for the three different configurations tested has been developed by Deaves [5], and the results are outlined below.

3.2.1. Single high-level opening

In this case, source gas will only emerge from the building if mixing is such that h_1 is equal to or exceeds the height of the opening. Since this is not the case for the runs undertaken, no gas will emerge, and this was noted in the tests. In general, if a layer of depth h_1 is formed by a release rate of Q_o ($m^3 s^{-1}$), the concentration is given by:

$$c = \frac{Q_o}{h_1 A} t \tag{6}$$

If this reaches a value of c_m before it begins to increase in height, and c_m then remains constant until the layer reaches the opening, it can be shown that no gas will emerge until

$$t_r = c_m \frac{V}{Q_o} \tag{7}$$

In the test cases considered, this timescale is not reached, and the build-up follows Eq. (6).

3.2.2. Single low-level opening

Gas/air mixture will always be emitted from a low-level opening, but will initially only be at a low concentration. The inflow is thus Q_o, and the leakage $Q_o c$, from which it can be shown that

$$c = 1 - \exp\left(\frac{-Q_o t}{h_1 A}\right) \tag{8}$$

For small values of $Q_o t/h_1 A$, this reduces to Eq. (6). For Runs 3–5, $Q_o = 0.01$ $m^3 s^{-1}$ and, from the measured results, $h_1 \simeq 1.4$ m. At the end of each test, $t = 300$ s, giving $Q_o t/h_1 A = 0.36$, which agrees with the final concentration for a high-level opening (Run 3), as presented in Table 2. Inserting this into Eq. (8) gives $c = 0.30$ as

the final concentration for the low-level opening (Run 5); the measured value (Table 2) is around 0.32.

3.2.3. Openings at both high and low level

In this case, the flow has a further transient component, relating to the magnitude of the volume outflow from the lower opening. Since the two openings are equal in area, the initial outflow will be $Q_o/2$ from each of the high- and low-level openings. As the gas concentration increases, a gravity driving force develops which alters the balance between these two openings. It is possible that, at some point, the flow at the top opening becomes zero, and the outflow from the lower opening is then Q_o. After this time, there will be inflow at the top, and the lower outflow will increase beyond Q_o, until a steady state is set up in which

$$Q_o = c_s Q_s \tag{9}$$

where

Q_s = steady − state volume outflow from lower opening ($> Q_o$)

c_s = steady − state concentration of mixed gas layer (< 1)

Applying standard ventilation principles for flows through these openings, and including the negative buoyancy driving force, it is possible to calculate both the steady-state values Q_s, and also the development in time of the layer concentration and of the outflow from the openings. The results are dependent on the layer depth, h_1, which is assumed, from the measurements, to be 1.4 m for Run 4 and 1.6 m for Run 7. The following definitions are used

$Q^* = Q_2/Q_o$ = normalised volume outflow

Q_2 = volume outflow from lower opening

c = concentration of mixed layer

Thus Q^* will increase from 0.5, where $c = 0$, to 1.0 at flow reversal, eventually reaching a steady-state value of Q_s.

4. CFD modelling

Although the measurements presented in Section 2 clearly provide useful detail on the gas build-up characteristics, their primary purpose was for the validation of results from CFD modelling. Various other CFD validation tests had already been investigated intensively by the authors (Gilham et al., [3]), with particular emphasis on the studies of contaminant flow coordinated by the International Energy Agency [6]. This programme included both flow and concentration measurements and CFD simulations, as described by Whittle [7]. These IEA test cases were used for a significant number of tests on aspects of mesh size, jet modelling, turbulence modelling etc. The results of these tests have been discussed in Gilham et al. [3] and conclusions on the approach which is appropriate to the modelling of the Silsoe case are summarised below.

(a) Mesh: A regular structured mesh is adequate, provided that the inlets, outlets, jets and obstructions are sufficiently well resolved. When using the κ–ϵ model with wall functions, checks on the near-wall grid spacing should also be made to ensure the validity of the model.

(b) Inlet and gas source conditions: Where inlets are of sufficient size, they should be modelled within the mesh. If necessary, however, sub-grid modelling can be used, provided that appropriate source terms are added to the turbulence equations.

(c) Turbulence modelling: It has been shown that the κ–ϵ model is robust and also provides reasonable predictions of the gas build-up and dispersion in enclosed volumes. The renormalisation group theory modification (RNG) was found to have little effect on the results, whilst the two-layer model was only found to be necessary for the resolution of wall jets. The standard κ–ϵ model was therefore used for the test cases presented here.

4.1. Cases studied

The test runs presented in Section 2 have demonstrated that the configuration of the outlets, whether high (U), low (L), or both (U + L) have little effect on the nature of the gas build-up, whereas the inlet flow rate does affect the results. It was therefore decided to apply CFD modelling only to those cases in which only the upper outlet was open; i.e. Runs 3 and 8.

4.2. CFD code

Whilst it is possible to adapt research CFD codes and tune them to specific classes of problems, it was decided to use a standard commercial package. Several such packages are available, most of which offer similar ranges of features for meshing, solving and turbulence modelling. A review at an earlier stage of the HSE study identified STAR-CD [8] as a suitable code, and this was used for the results presented here. A summary of the features rendering STAR-CD particularly useful for the applications considered is presented below:

- Mesh generation — allows local mesh embedding.
- Solver — uses efficient PISO solver.

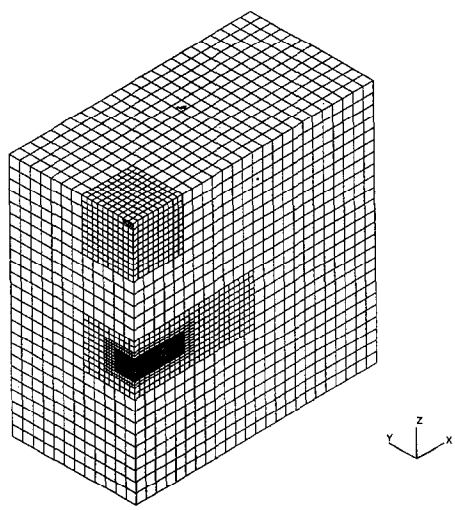

Fig. 6. Computational mesh structure.

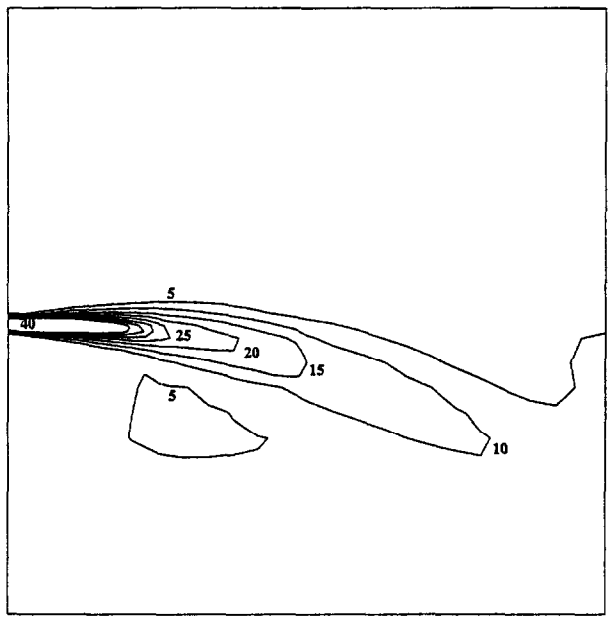

a) after 60 seconds

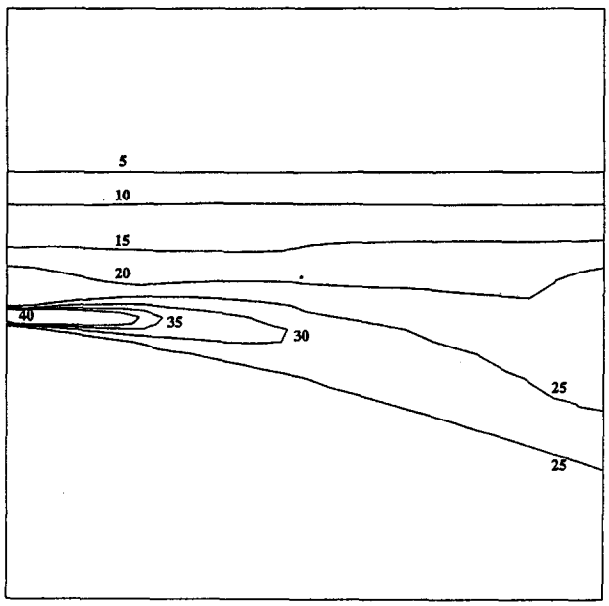

b) after 300 seconds

Fig. 7. Computed CO_2 concentration contours for Run 3, 70% concentration at 600 $l min^{-1}$, upper vent only open.

- Turbulence modelling — range of models available.
- Post-processing — efficient post-processing analysis capabilities.

The code was used with the approach noted above; further details specific to these tests are given below.

4.3. Mesh

The obtaining of good results from CFD studies is dependent upon specifying an appropriate mesh to resolve the flows in the areas of interest. Related work presented by Gilham et al. [3] undertook mesh-dependency studies for the application of CFD methods using the κ–ϵ turbulence model within similar cuboid enclosures to that studied here. The results of these studies were used to set the meshing for the CFD runs reported here.

The simplicity of the geometry allows the use of a straightforward rectangular mesh as a basis for the computations. In view of the symmetry of the flow, only half the domain is modelled, using a basic mesh of 0.1 m in each direction, giving $24 \times 24 \times 12$

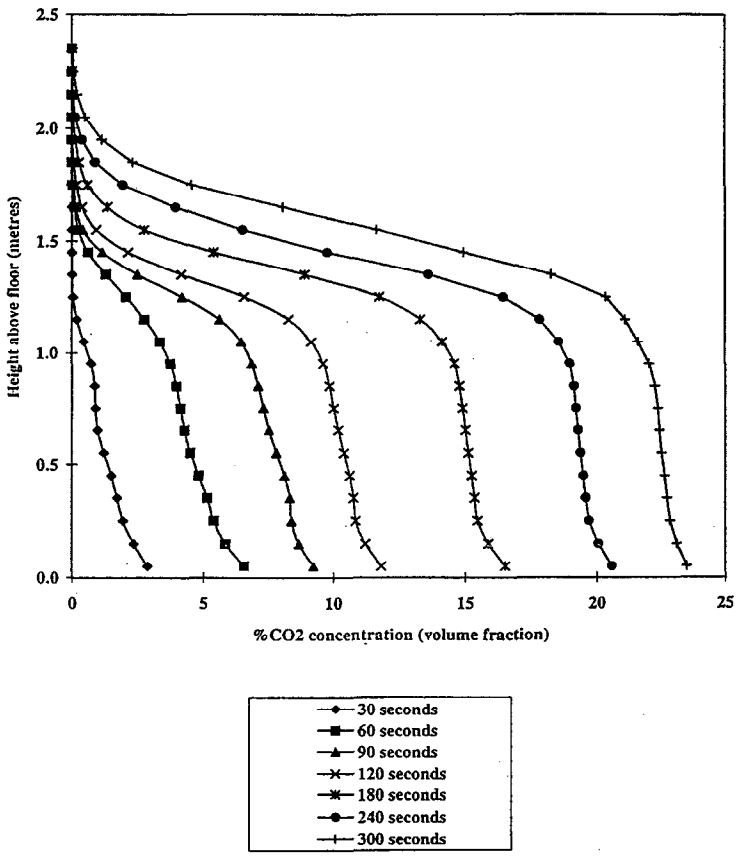

Fig. 8. Computed CO_2 concentration profiles at the sensor location, 70% concentration at 600 $l min^{-1}$, upper vent only open.

nodes. The only significant features which need to be resolved beyond this level of detail are the inlet orifice (50 mm diameter) and the outlet slot at the top of the room (50 × 200 mm). These were resolved by embedding a refined mesh of 0.05 × 0.05 m near the outlet, and a mesh which is variably refined down to 0.01 × 0.025 m near the gas inlet. The mesh consists of 13 000 modes in total, and its structure is shown in Fig. 6.

4.4. Numerical scheme

The efficient PISO solver is used, together with the SCFD discretisation scheme. This was found, from previous test cases, to give robust and efficient solutions.

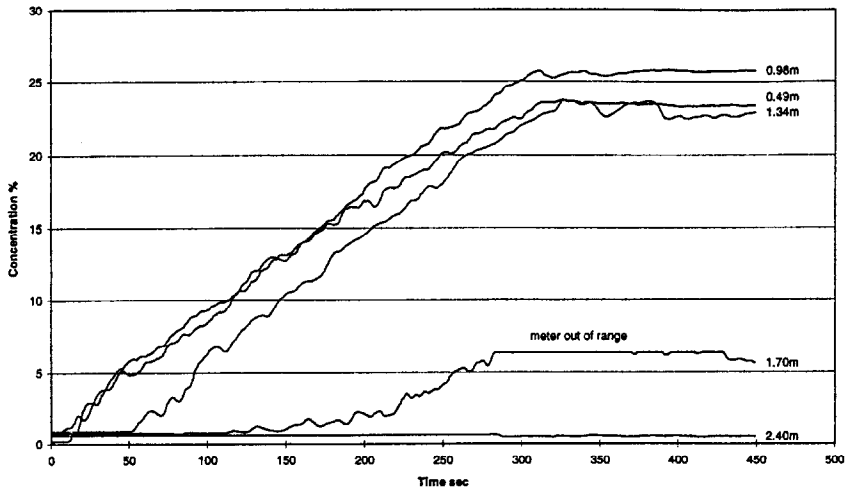

a) **Experimental Results**

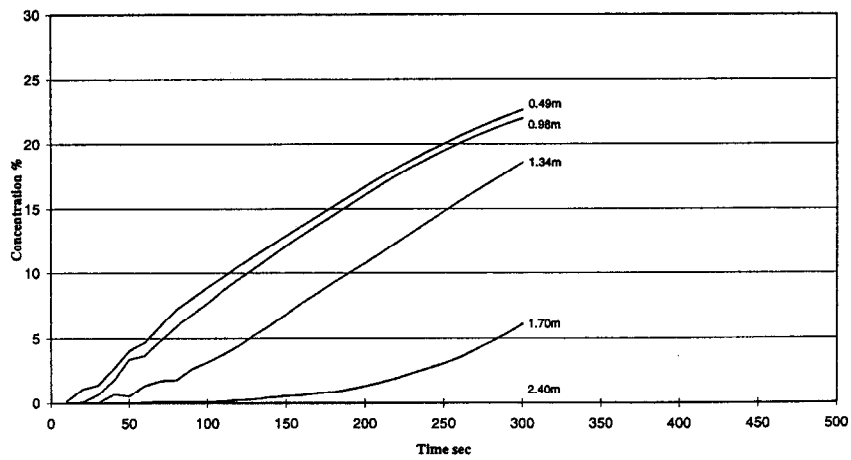

b) **Computed Results**

Fig. 9. CO_2 concentration time history for Run 3.

4.5. Turbulence modelling

The standard κ–ϵ model is used, with wall functions to ensure appropriate modelling near the boundaries. Use of these functions requires that values of the near-wall length parameter, y^+, do not become too large. These have been checked at various stages of the calculation, and found generally to be within the appropriate limits.

4.6. Boundary conditions

Walls of enclosure: non-slip boundaries with wall functions as noted above.

Symmetry plane: zero flux.

Gas inlet: specified velocity (5 $m\,s^{-1}$, 8 $m\,s^{-1}$), turbulence kinetic energy (0.375 $m^2\,s^{-2}$, 0.96 $m^2\,s^{-2}$) and gas concentration, (70%, 80%). Values quoted are for Runs 3 and 8, respectively.

Relief outlet: zero gradient for all quantities.

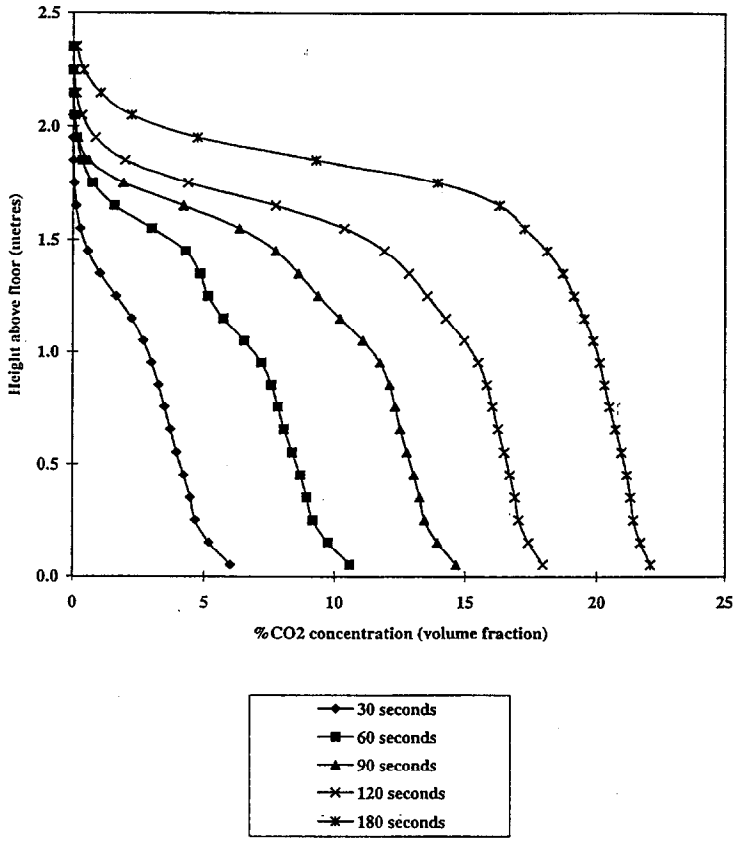

Fig. 10. Computed CO_2 concentration profiles at the sensor location, 70% concentration at 950 $l\,min^{-1}$, upper vent only open.

4.7. Results

For Run 3, the CFD code was run for the full length of the transient (300 s), with a time step of 1 s. Two-dimensional views of the concentration build-up on a vertical plane through the jet axis are presented in Fig. 7a and Fig. 7b for 60 s and 300 s, respectively. The downward sinking of the jet caused by the CO_2 density is clearly evident in Fig. 7a, and compares well with the flow visualisation results shown in Fig. 2. As the density of the lower layer increases, so the density difference between the jet and its surroundings decreases, resulting in rather less sinking, as can be seen in Fig. 7b.

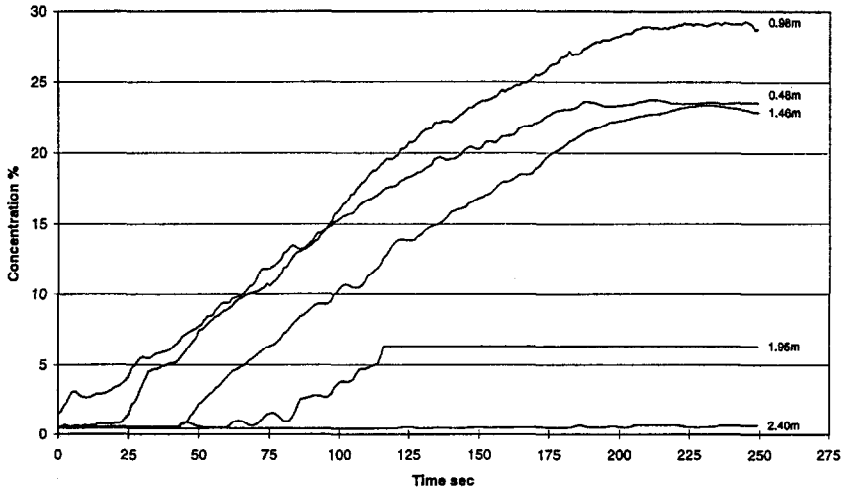

a) **Experimental Results**

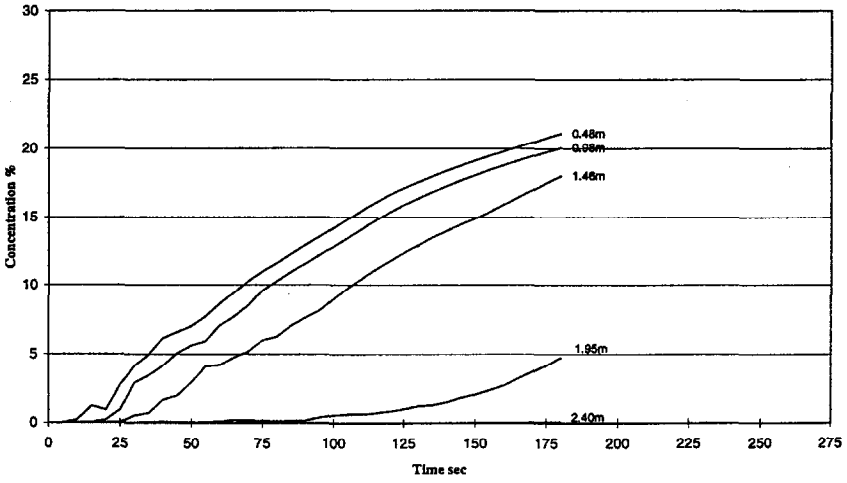

b) **Computed Results**

Fig. 11. CO_2 concentration time history for Run 8.

Concentration results are presented at various times from 30 to 300 s in Fig. 8. This shows the progression to a fairly uniformly mixed layer with the concentration decreasing to zero across the top 0.5 m or so of the layer. The gas build-up with time is shown in Fig. 9, which also provides a comparison with the corresponding measurements, and shows that the predicted behaviour matches very well to the test results. The comparison is discussed further in Section 5.

For Run 8, the transient lasts only 180 s. Again, the full length of this transient was modelled with a time step of 1 s. Concentration results are presented for various times from 30 to 180 s in Fig. 10. The results show similar features to those identified for Run 3. In this case, however, the higher momentum of the jet results in rather less 'sinking' due to the density of the CO_2. In addition, the rather greater jet effects cause a deeper layer and a broader edge region through which the concentration drops to zero. The gas build-up with time is shown in Fig. 11. This also provides a comparison with the corresponding measurements, which again is discussed below.

5. Comparisons between various modelling approaches

5.1. Simple vs. physical modelling

Runs 3 and 8 both only have vents at the top, resulting in a linear build-up of concentration with time. The more interesting results, in which outflow rates from the vents are not so clearly defined, are those for which both vents are open, Runs 4 and 7. Using the notation set out in Section 3, the following are the calculated sequences of (c, Q^*) values from commencement to steady state (c_s, Q_s^*):

Run 4 (c,Q^*): (0, 0.5) → (0.1, 1.0) → (0.51, 1.96)

Run 7 (c,Q^*): (0, 0.5) → (0.21, 1.0) → (0.64, 1.56)

The sequence in each case is: flow from both openings → flow reversal at top opening → steady-state flow from bottom opening.

The normalised final concentration for each run has been presented in Table 2. It is clear, from the measured concentrations, that the final steady states indicated above have not been reached during the relatively short timescale of the releases. If it is then assumed that Q^* is a linear function of c for each distinct phase of the transient, the flow-reversal timescales can be calculated as 90 s for Run 4 and 131 s for Run 7. The variation of concentration with time for these runs is shown in Fig. 12a and Fig. 12b, respectively.

When considering these plots, it should be noted that the simple model results are based on the assumption of a uniform concentration throughout the mixed layer. The results will also depend upon the layer depth which has been used, and would, for example, be closer to the experimental data for Run 4 if a slightly lower depth (< 1.4 m) was used. With these reservations, it can be seen that there is reasonable agreement between model and experiments. Although model constants can clearly be adjusted to achieve a 'good fit', closer examination of the results for Run 7 (Fig. 12b) does suggest that the change in slope of the concentration vs. time plot at flow reversal ($t = 131$ s) is a real feature of the measurements. The sudden change of slope observed on these plots is partly dependent upon the modelling assumption that flow reversal, when it happens,

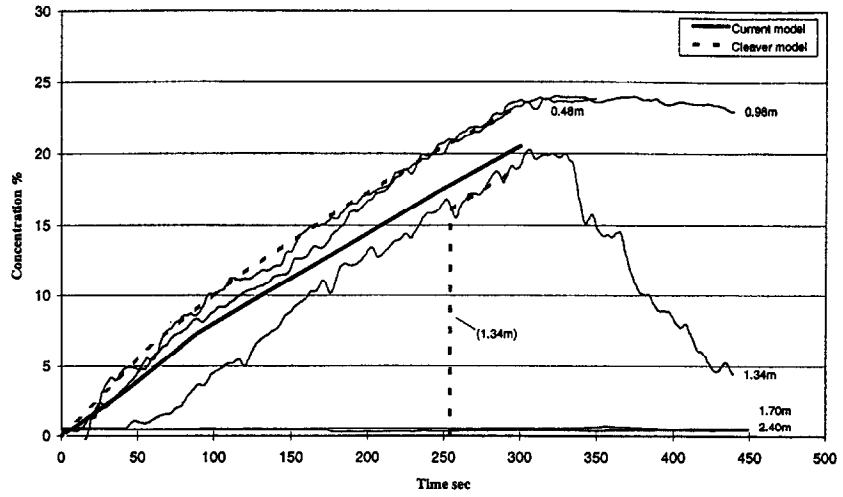

a) Run 4

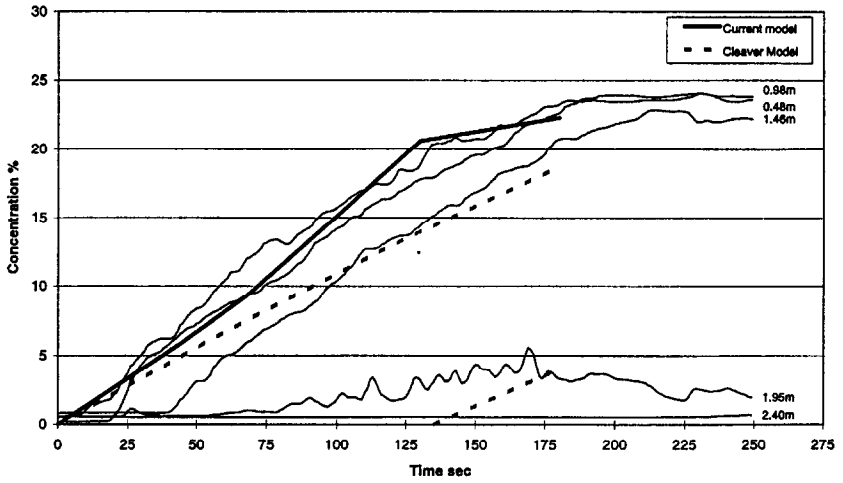

b) Run 7

Fig. 12. Comparison of simple model predictions with experimental results for: (a) Run 4, and (b) Run 7.

is instantaneous. In practice, there may be a finite transition time such that this change in slope is less abrupt. For the current tests, the small vent sizes will minimise any such smearing effect.

The simple model used in the comparisons is designed to allow the prediction of release rates from the building. The internal stratified structure is therefore modelled in a simplified manner such that the layer depth is assumed constant. The model of Cleaver et al. [4] represents the internal structure in a more realistic manner, allowing (in the

case of a dense gas) a fixed depth lower layer above which is a growing upper layer, each of which has its own average concentration which is increasing with time.

Some results from this model (extended to allow for the effects of the ventilation outlets) have been made available to the authors, and are included on Fig. 12. The model predicts that the measuring positions at the lower elevations in both Runs 4 and 7 were within the bottom well-mixed layer and the concentrations predicted by the model at these locations are in agreement with the observations. The growth rate of the upper layer is slightly underpredicted by the model, with the result that the observed gradual rise in concentration after approximately 40 s at 1.34 m elevation in Run 4 and after 80 s at 1.95 m in Run 7 is not reproduced. For comparison, the upper layer is predicted to have reached an elevation of 1.17 m after 40 s in Run 4 and an elevation of 1.89 m after 80 s in Run 7. The growing layer is predicted to arrive at an elevation of 1.34 m after 254 s in Run 4 and 1.95 m after 135 s in Run 7. Thereafter, the associated concentrations are again in agreement with the measurements, as shown in Fig. 12.

5.2. CFD vs. physical modelling

The layer depth does not have to be defined a priori in the CFD modelling, enabling direct comparisons to be made with no adjustment. These are presented in Figs. 9 and 11 for Runs 3 and 8, respectively, from which it can be seen that there is good agreement between the results. The main differences in both cases can be attributed to the higher concentrations recorded at 0.98 m than those at 0.49 m. However, it does appear from the reasonable agreement at each measurement height that the CFD results have, in each case, successfully predicted the position and extent of the interface at the top of the mixed gas layer.

6. Conclusions

For the releases considered, where the jet momentum is significant, but not dominant, it has been shown that, for a denser-than-air release, a distinct lower well-mixed layer develops whose depth remains fairly constant with time, but whose concentration increases linearly while gas is being injected. There is also some evidence, both from the experimental measurements and the mathematical modelling results, for the existence of an overlying stratified layer that grows with time. The experimental results also show that, for the relatively small ventilation slots used, their configuration has only a minor effect on the results.

It has been shown that simple 'zone' type modelling can be applied to this problem, and can be matched to the experimental results. The main problem from the modelling point of view is that the depth of the mixed layer needs to be fixed a priori, and this is found, from the work of Cleaver et al., to be extremely sensitive to the exact jet effects in the cases studied here, and, to some extent, on the interpretation of Cleaver's method.

CFD modelling has been successfully applied to two of the test cases, and has been shown to give good qualitative and quantitative agreement. It is emphasised, however, that significant background effort in determining appropriate meshing and boundary conditions was applied before undertaking these runs. In general, considerable care is therefore needed in applying CFD in a genuinely predictive manner.

In spite of the sensitivity of 'simple modelling' in the cases considered, it appears to offer a useful tool in determining gas releases from buildings. For example, it can be shown that the outflow from a building may be significantly reduced if mixing is incomplete. In view of the success of CFD in this case, it is possible that the major drawback of such models — the uncertainties in mixed layer depth — could be further investigated by the application of a more extensive series of CFD test runs.

Acknowledgements

The authors wish to thank Dr. R.P. Cleaver of British Gas for his helpful comments on the text, and for making available the results from his model for comparison with these experimental results. All the work reported here was funded by the Major Hazards Assessment Unit of the UK Health and Safety Executive.

References

[1] R.C. Hall, P. Gallagher, M.T.G. Harris and D.M. Deaves, Health and Safety Executive Contract Research Report No. 75/1995, Her Majesty's Stationary Office, 1995.
[2] P.W.M. Brighton, Heavy-gas dispersion from sources inside buildings or in their wakes, IChemE North Western Branch Symposium, Refinement of Estimates of the Consequences of Heavy Toxic Vapour Releases, UMIST, Manchester, 8 January 1986.
[3] S. Gilham, S. Ferguson and D.M. Deaves, Dispersion of releases of hazardous materials within buildings — Phase II, CFD modelling, Health and Safety Executive Contract Research Report No. RSU8000/012/1, Her Majesty's Stationary Office, 1996.
[4] R.P. Cleaver, M.R. Marshall and P.F. Linden, The build up of concentration within a single enclosed volume following a release of natural gas, J. of Hazardous Materials, 36 (1994) 209–226.
[5] D.M. Deaves, Simple modelling of gas release from buildings, Health and Safety Executive Contract Research Report No. RSU 8000/012/2, Her Majesty's Stationary Office, 1995.
[6] A.D. Lemaire (Ed.), Room Air and Contaminant Flow, Evaluation of Computational Methods, Subtask-1 Summary Report, IEA Annex 20, 1992.
[7] G. Whittle, Evaluation of measured and computer test case results from Annex 20, Subtask 1, 12th AIVC Conf. Air Movement and Ventilation Control within Buildings, Ottawa, Canada, 24–27 September 1991.
[8] STAR-CD, Version 2.2 Manuals, Computational Dynamics, London, 1994.